Multiple phosphate positions in the catalytic site of glycogen phosphorylase: Structure of the pyridoxal-5′-pyrophosphate coenzyme-substrate analog

ARTICLE *in* PROTEIN SCIENCE · SEPTEMBER 1992

Impact Factor: 2.85 · DOI: 10.1002/pro.5560010904 · Source: PubMed

3 AUTHORS, INCLUDING:

Stephen G Withers
University of British Columbia - Vancouver
573 PUBLICATIONS **19,943** CITATIONS

Protein Science (1992), *1*, 1100–1111. Cambridge University Press. Printed in the USA.

Multiple phosphate positions in the catalytic site of glycogen phosphorylase: Structure of the pyridoxal-5′-pyrophosphate coenzyme–substrate analog

STEPHEN R. SPRANG,[1] NEIL B. MADSEN,[2] AND STEPHEN G. WITHERS[3]

[1] Howard Hughes Medical Institute and Department of Biochemistry, The University of Texas Southwestern Medical Center, Dallas, Texas 75235-9050
[2] Department of Biochemistry, University of Alberta, Edmonton, Alberta T6G 2H7, Canada
[3] Department of Chemistry, University of British Columbia, Vancouver, British Columbia V6T 1Z1, Canada

(RECEIVED December 24, 1991; REVISED MANUSCRIPT RECEIVED March 9, 1992)

Abstract

The three-dimensional structure of an R-state conformer of glycogen phosphorylase containing the coenzyme–substrate analog pyridoxal-5′-diphosphate at the catalytic site (PLPP-GPb) has been refined by X-ray crystallography to a resolution of 2.87 Å. The molecule comprises four subunits of phosphorylase related by approximate 222 symmetry. Whereas the quaternary structure of R-state PLPP-GPb is similar to that of phosphorylase crystallized in the presence of ammonium sulfate (Barford, D. & Johnson, L.N., 1989, *Nature 340*, 609–616), the tertiary structures differ in that the two domains of the PLPP-GPb subunits are rotated apart by 5° relative to the T-state conformation. Global differences among the four subunits suggest that the major domains of the phosphorylase subunit are connected by a flexible hinge. The two different positions observed for the terminal phosphate of the PLPP are interpreted as distinct phosphate subsites that may be occupied at different points along the reaction pathway. The structural basis for the unique ability of R-state dimers to form tetramers results from the orientation of subunits with respect to the dyad axis of the dimer. Residues in opposing dimers are in proper registration to form tetramers only in the R-state.

Keywords: active site; allosteric control; enzyme mechanism; glycogen; glycogen phosphorylase; phosphorolysis; pyridoxal diphosphate; pyridoxal phosphate; R-state

Glycogen phosphorylase (EC 2.4.1.1) catalyzes the phosphorolytic degradation of glycogen, thereby generating the G-1-P required to meet metabolic energy requirements and maintain glucose homeostasis. Homologs of this enzyme are present in diverse species ranging from yeast to human (Newgard et al., 1989); many of the eukaryotic enzymes function as cooperative homodimers and are regulated by phosphorylation and by allosteric effectors. All α-D-glucan phosphorylases, however, are dependent for their activity on a covalently bound PLP coenzyme (Graves & Wang, 1972). The aldehyde group of the pyridoxal forms a Schiff base linkage to the ε-amino group of lysine 680 that is stable under physiological conditions. The discovery (Fischer et al., 1958) that the Schiff base linkage could be reduced without substantial loss of activity suggested that the catalytic role of the pyridoxal in phosphorylase is quite different from that in other B6-dependent enzymes. Experiments with coenzyme analogs (Shaltiel et al., 1969; Graves & Wang, 1972; Pfeuffer et al., 1972; Parrish et al., 1977) identified the phosphate group of the PLP as the critical catalytic moiety.

It is now well established by kinetic, NMR, and crystallographic studies that the PLP phosphate participates in catalysis through a direct, noncovalent contact with the phosphate substrate or the phosphate group of the G-1-P product (Withers et al., 1981b; Takagi et al., 1982; Klein et al., 1982, 1986; McLaughlin et al., 1984). Key pieces of evidence included the finding that when PLP is replaced by the coenzyme–substrate analog, PLPP, the resultant inactive enzyme is locked into an R-state conformation

Reprint requests to: Stephen R. Sprang, Howard Hughes Medical Institute and Department of Biochemistry, The University of Texas Southwestern Medical Center, Dallas, Texas 75235-9050.

Abbreviations: GPb and GPb, glycogen phosphorylase b and a; PLP, pyridoxal phosphate; PLPP, pyridoxal-5′-pyrophosphate (or 5′-diphosphate); PLPPGlu, pyridoxal-5′-diphospho-1-α-D-glucose; GCP, α-D-glucose-1,2-cyclic phosphate; G-1-P, α-D-glucose-1-phosphate.

in the presence of AMP (Withers et al., 1982b). In addition, reconstitution of apophosphorylase with the alternate coenzyme–substrate analog, PLPPGlu yields an enzyme capable of a single stereospecific glucosyl transfer to glycogen, generating PLPP at the active site.

The nature of the contact between the substrate and coenzyme phosphate groups and the mechanism by which it facilitates catalysis is not well established. Two proposals have been advanced to explain the catalytic role of the PLP phosphate. Helmreich et al. (1980) and Klein et al. (1982, 1986) postulated that the PLP acts as a general acid–base catalyst in the protonation/deprotonation of the substrate phosphate or the G-1-P phosphate. In contrast, Madsen, Withers, and Fukui have suggested that the coenzyme phosphate moiety is tightly constrained in the transition state and adopts a distorted bipyramidal configuration (Withers et al., 1981a,b). The constrained dianion is proposed to act as an electrophilic catalyst by recruiting an oxygen atom of the leaving group phosphate as a fifth ligand.

Both of the catalytic mechanisms proposed for glycogen phosphorylase require the close approximation of the substrate and coenzyme phosphate groups in an oriented complex. The PLPP-GPb moiety mimics to differing extents the phosphate–phosphate interactions proposed for these two mechanisms. The 2.5-Å P–P distance in PLPP approximates that expected for a bipyramidal transition state, although the configuration about the 5′ phosphate in PLPP is tetrahedral rather than bipyramidal. PLPP is a less faithful mimic of a hydrogen-bonded phosphate–phosphate complex in which the two phosphates would be separated by at least 4.5 Å. Nevertheless, it is expected that the PLPP pyrophosphate group would partially overlap the two subsites that would be occupied by a hydrogen-bonded phosphate pair.

The access of substrates to the catalytic site of phosphorylase is regulated by the conformational state of the enzyme (Barford & Johnson, 1989; Sprang et al., 1991). Glycogen phosphorylase is a cooperative homodimer that may be approximately described in terms of the Monod–Wyman–Changeux model (Monod et al., 1965) as an equilibrium population of inactive T-state and active R-state conformers (Buc, 1967). AMP binds to a regulatory site at the subunit interface (Kasvinsky et al., 1978b; Lorek et al., 1984; Sprang et al., 1987, 1988, 1991) and drives the dephosphorylated enzyme (phosphorylase b or GPb) toward the R-state. Phosphorylation at Ser 14 produces an active enzyme (phosphorylase a, or GPa) that does not require AMP for activity and binds both AMP and substrates noncooperatively with high affinity (Fletterick & Madsen, 1980). Crystallographic studies of both GPb (Barford & Johnson, 1989; Acharya et al., 1991) and GPa (Sprang & Fletterick, 1979; Sprang et al., 1987, 1991; Withers et al., 1982a; Goldsmith et al., 1989b) bound to a variety of regulatory ligands have revealed a spectrum of conformational substrates, suggesting that a two-state model does not accurately describe the range of structures accessible to the enzyme.

PLPP-GPb is poised slightly closer to the activated R-state conformation than the PLP enzyme in the presence of G-1-P. The PLPP enzyme binds adenosine 5′-monothiophosphate with a dissociation constant, K_d, of 40 μM, which is comparable to that of GPb ($K_d = 140$ μM) in the presence of saturating G-1-P. The PLPP enzyme is dimeric in the absence of ligands, characteristic of the inactive T-state, but is converted to tetramers in the presence of AMP (Withers et al., 1982b). Crystals of tetrameric PLPP-GPb bound to AMP have been obtained by precipitation from polyethylene glycol. The X-ray structure of PLPP-GPb resolved at 3.0 Å (Sprang et al., 1991) reveals a tetrameric R-state enzyme similar but not identical to that of sulfate-activated GPb (Barford & Johnson, 1989).

The PLPP enzyme serves as a model of the catalytically active R-state of GP. In this report, we describe briefly the mechanism by which the T → R transition induces the formation of tetramers and suggest why tetramers dissociate in the presence of glycogen. Our primary focus, however, is the catalytic site of PLPP-GPb as a model of the R-state enzyme–substrate complex. We describe the stereochemistry of the PLPP moiety as a model of the putative complex formed by the substrate and coenzyme phosphates in the course of catalysis. The refined 2.87-Å resolution structure shows that the terminal phosphate group of the modified coenzyme adopts two conformations that may mimic discrete states in the catalytic cycle of the enzyme. A parallel study of PLPP-GPb crystallized in ammonium sulfate by Leonidas et al. is described in an accompanying paper (Leonidas et al., 1992).

Results

The crystallization of the complex of PLPP-GPb with AMP and the determination of its three-dimensional structure at 3.0 Å has been described (Sprang et al., 1991). The crystallographic refinement has now been extended to include diffraction data extending to 2.87 Å resolution. A summary of data collection and refinement statistics is presented in Table 1.

The asymmetric unit contains four subunits of PLPP-GPb related by noncrystallographic 222 symmetry. Superposition of corresponding Cα atoms of the four subunits reveals an average root mean square (rms) difference of 0.62 Å, which is about twice the estimated accuracy of the coordinates as estimated by the method of Luzzati (1952). The differences are nonrandom and appear to have a structural basis as discussed below. Examination of the 2Fo − Fc map computed after the first cycle of refinement with 2.87 Å data revealed two conformations for the PLPP in subunits A and C. Trial positions for these residues were obtained by fitting PLPP fragments to "simulated annealing omit" electron density maps (Brünger, 1990) in which phase bias from the PLPP and

Table 1. *Crystal parameters,*[a] *crystallographic data, and refinement statistics for PLPP-GPb*

Data statistics	
Reflections $I > 3\sigma(i)$ (no.)	93,184
Complete at 2.87 Å (%)	90.1
Rmerge[b]	0.065
Refinement statistics	
Atoms (no.)	26,226
Rcryst (8–2.87 Å)	0.185
Rcryst (∞–2.87 Å)	0.22
rms deviation from ideal	
Bond lengths (Å)	0.014
Bond angles (degrees)	3.2

[a] The space group is $P2_12_12$; cell constants a = 169.9 Å, b = 209.9 Å, and c = 123.4 Å. There are 16 subunits/cell, and the protein content is 43%.

[b] Merging R is defined as: $Rmerge = \Sigma_h \Sigma_i |I(h) - I_i(h)| / \Sigma_h \Sigma_i I_i(h)$, where $I_i(h)$ and $I(h)$ are the ith and the mean measurement of the intensity of reflection h, respectively. The crystallographic R value is $Rcryst = \Sigma_h [|Fobs(h) - Fcal(h)| / \Sigma_h Fobs(h)]$, where $Fobs(h)$ and $Fcal(h)$ are the observed and calculated structure factor amplitudes, respectively.

its immediate surroundings is minimized. Alternative positions for the PLPP side chains were refined independently. The electron density in the region of the PLPP side chain is shown for all four subunits in Figure 1. The side chain atoms for Arg 569 were found to be disordered. In simulated annealing omit maps from which Arg 569 was excluded from the phase calculation, no electron density was observed beyond the Cδ atom of Arg 569 in any of the four subunits.

The refined model comprises, for each of the four subunits, residues 10–247, 266–276, 289–837, the two positions for the PLPP moieties (subunits A and C only), and one molecule of AMP. In subunit B, residues 10–19 are not visible. Lattice contacts, unique to the B subunit, are presumed to prevent these residues from adopting the ordered conformation observed in the other three subunits. No identifiable electron density corresponding to the maltoheptaose was found either at the catalytic site or glycogen storage sites even though crystals were grown in the presence of high (12.5 mM) oligosaccharide concentration. The final crystallographic R-factor for all data between 8.0 and 2.87 Å resolution is 0.185.

Tetramer contacts

The most extensive intersubunit contacts are those that stabilize the catalytically functional dimers: subunits A/B and C/D (pairs related by the molecular p axis in the nomenclature of Barford & Johnson [1992]). The latter mediate cooperativity between subunits and have been described in detail (Sprang & Fletterick, 1979; Sprang et al., 1988, 1991; Acharya et al., 1991; Barford et al., 1991). Tetramers are stabilized primarily by polar interactions between residues on the catalytic faces of op-

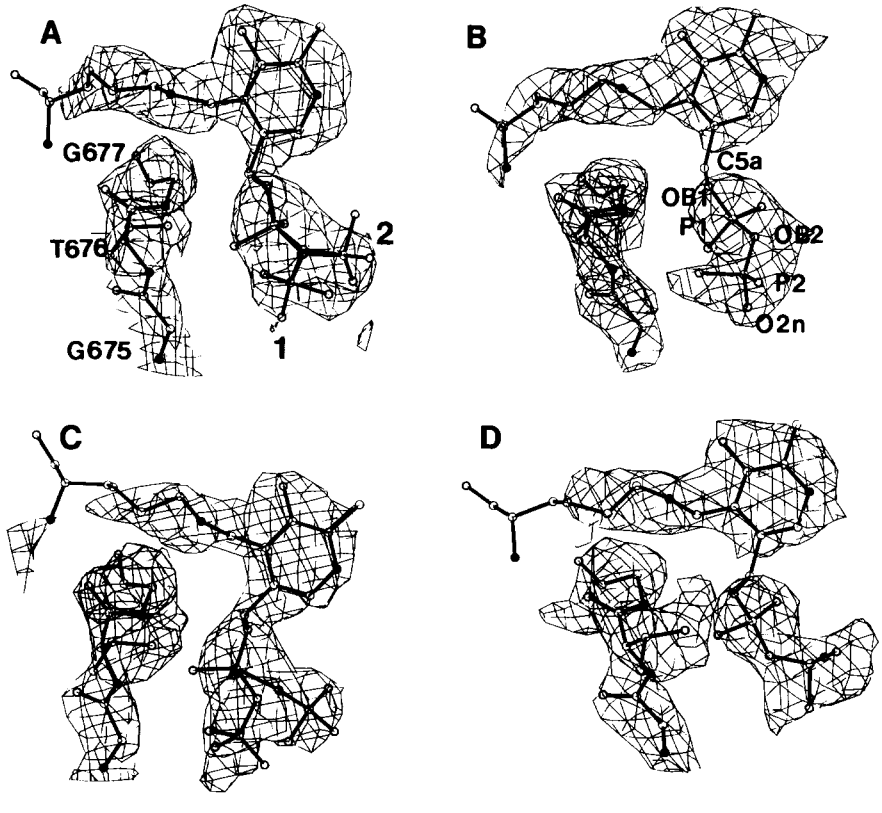

Fig. 1. The 2Fobs – Fcalc electron density map calculated with refined phases for data between 8.0 and 2.87 Å resolution, contoured at 1.2 standard deviations above the mean value of the map. The map volumes shown enclose the PLPP cofactor analog in each of the four subunits. Both conformations are depicted for the coenzyme in subunits A and C. Residues 675–677 are identified for subunit A, as are the two positions observed for the terminal phosphate of PLPP. The naming convention for the PLPP phosphodiester backbone is shown for the coenzyme in subunit B.

posing A/B and C/D dimers. The contacting residues are grouped into four clusters on the face of the subunit (Fig. 2a).

Most of the dimer–dimer interface is formed by contacts between subunits A and D (equivalently, between B and C) related by the *q* axis (Barford & Johnson, 1992). Prominent among these are the contacts at the oligosaccharide binding site. Here, Arg 426 and Glu 433 in subunit A form an ion pair and a hydrogen bond, respectively, with Asp 756 and Gln 754 at the C-terminus of helix 17 in the C-terminal domain (residues 486–842) of subunit D (secondary structure designations follow the convention of Acharya et al. [1991]) (Fig. 2b). The intramolecular ion pair between Arg 426 and Asp 422 observed in crystals of glucose-inhibited GPa is maintained in the R-state PLPP-GPb crystals. At the second major contact locus in the A/D interface, the side chain NH_2 groups of Gln 729 and Asn 727, which reside in a short β-strand following helix 23 in subunit A, form hydrogen bonds with the carbonyl oxygen atoms at the C-terminus of helix 23 in subunit D. The *q* dyad axis (Barford & Johnson, 1992) relating the dimers is in close proximity to and passes between residues 727 of subunits A and D (Fig. 2d). Valine 266 and Leu 267 at the N-terminus in the tower (α7) helix of subunit A forms a hydrophobic contact surface with the corresponding residues in subunit D.

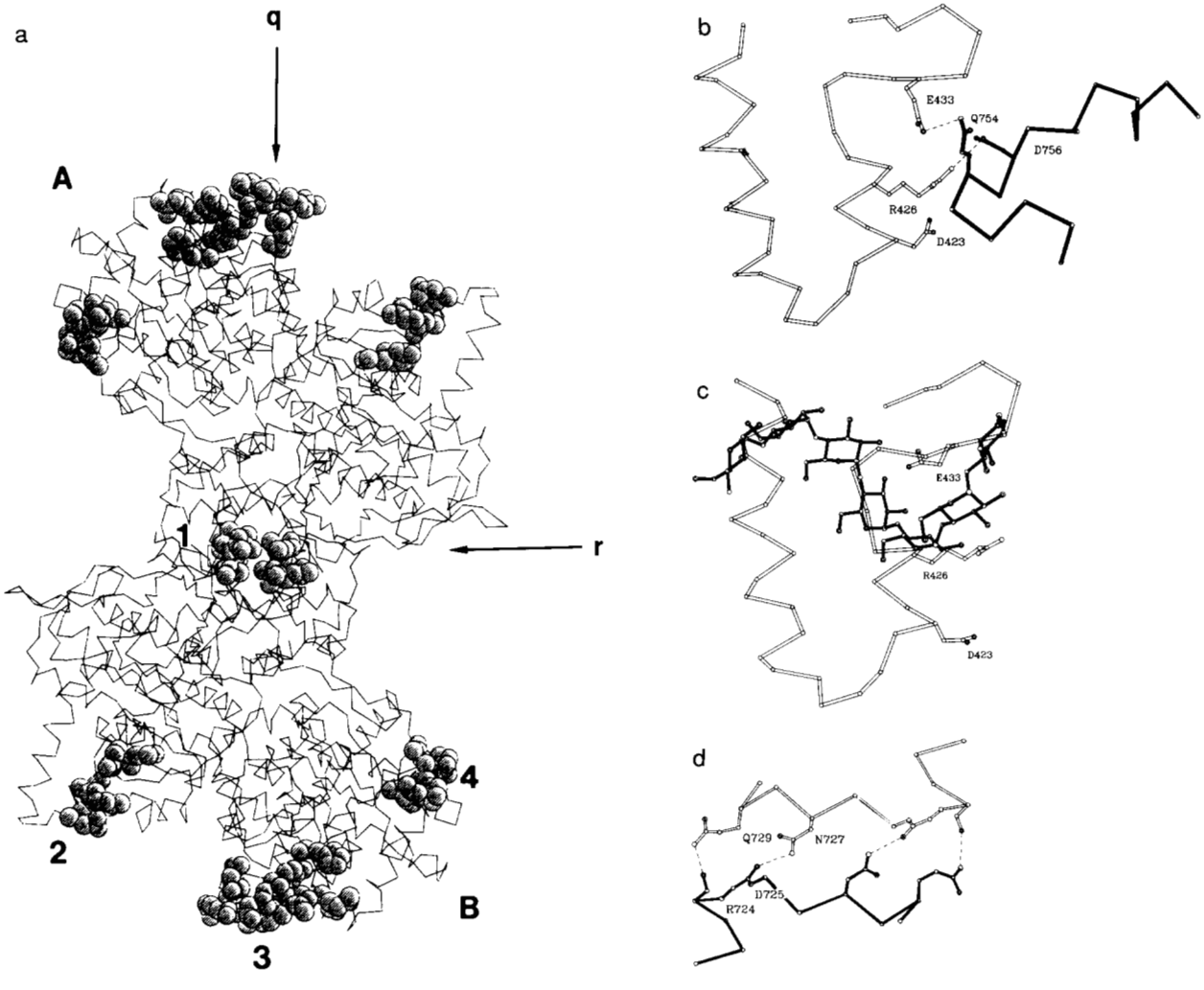

Fig. 2. Dimer–dimer contacts at the glycogen storage site. **a**: The catalytic dimer of PLPP-GPb viewed along the *p* dyad axis of the dimer (subunits A/B and C/D) toward the catalytic sites. Van der Waals spheres are shown for four clusters of residues involved in dimer–dimer contacts: Cluster 1, residues 264–267; cluster 2, residues 423–426, 433, and 434; cluster 3, residues 722–729; cluster 4: 753–757. Residues in cluster 2 of subunits A and B interact with residues in cluster 4 of residues D and C, respectively. Residues in cluster 3 of subunits A and D contact cluster 3 residues in subunits D and C, respectively. Cluster 1 residues of all four subunits are in mutual contact. **b**: Cluster 2–cluster 4 tetramer contacts: a Cα tracing of residues 403–434 in subunit A (empty bonds) and 749–759 in subunit D (darkened bonds). The intersubunit ion pair between Arg 426 and Asp 756 and the hydrogen bond between Glu 433 and Gln 754 are shown. **c**: The corresponding site in the complex between GPa and maltoheptaose (Goldsmith et al., 1989a). **d**: A view along the *q* axis showing cluster 3–cluster 3 contacts: the dyad-related contacts between residues 723 and 729 of subunit A (open bonds) and the corresponding residues in subunit D.

The interface between subunits A and C (equivalently, B and D) related by the molecular *r* axis (Barford & Johnson, 1992) is relatively small. A hydrogen bond is formed between Gln 264 and its *r*-axis-related counterpart. Thus, the N-termini of the tower helices of all four subunits interact on tetramer formation. The second interaction occurs between the outer strands, $\beta 8$, of the twisted antiparallel β-ribbons (residues 198–223), that overlie the glycogen storage sites of subunits A and C. Here there is a parallel stacking interaction between *r*-axis-related arginines 205 in which the planes of the guanidinium groups overlap and are separated by 4 Å. The charge associated with these residues is compensated by intrasubunit ion pairs with Glu 207. Subunit contacts in crystals of GPb obtained from ammonium sulfate have been described in detail by Barford and Johnson (1992) and are similar to those in PLPP-GPb tetramers.

A model-building experiment, conducted by superimposing dimers of glucose-inhibited (T-state-like) GPa onto the A/B and C/D dimers of PLPP-GPb (using residues 426–433 and 750–760) demonstrates that the structural elements that participate in the PLPP-GPb dimer–dimer contacts (clusters 2 and 4 in Fig. 2a) are not properly aligned to form such contacts in the T-state conformation. The superposition as performed above also shows potential steric conflicts between the helix 23 pair (cluster 3, Fig. 2a) that would be brought together as a result of tetramer formation. The 5° rotation of subunit A with respect to subunit B (and of C with respect to D), which accompanies the transition to the active conformation, positions the charged and polar side chains for optimal contact between dimers, thus allowing the tetramer formation. The absence of dimer–dimer interactions in the T-state precludes positive cooperativity within tetramers.

Glycogen induces the dissociation of R-state phosphorylase tetramers into catalytically active dimers (Wang et al., 1965; Metzger et al., 1967). Combined kinetic and crystallographic studies of GPa demonstrated that phosphorylase contains an oligosaccharide storage site distinct from the catalytic site, to which glycogen is bound with high affinity (Kasvinsky et al., 1978a). The storage site is located in a compact subdomain comprising residues 387–438 on the face of the subunit, which contains the active site. Crystallographic studies of α-(1,4)-linked D-glucosyl oligomers bound to GPa (Goldsmith et al., 1982, 1989a; Goldsmith & Fletterick, 1983) and GPb (Johnson et al., 1988, 1990) show that oligosaccharides adopt a left-handed helical conformation and bind to neighboring sites in the glycogen storage domain (Fig. 2c). The glycosyl residue that forms the largest number of contacts with the enzyme and has the lowest mean thermal parameter is bound in a shallow groove between the two helices, and forms hydrogen bonds with Glu 433 and Arg 426 (Goldsmith & Fletterick, 1983; Goldsmith et al., 1989a). Model building shows that although oligosaccharides such as maltoheptaose may not sterically block tetramer formation, they form their strongest interactions with the enzyme at the site involved in dimer–dimer contacts. Hence, glycogen might inhibit tetramer formation by competing for residues at the tetramer interface.

Structural changes on transition to the activated enzyme conformation

The differences between PLPP-GPb and the inactive T-state conformation of the enzyme have been described (Sprang et al., 1991). Two major transformations that accompany the transition from the inactive T-state to the catalytically active R-state were reported. The first, previously observed in crystals of sulfate-activated GPb and GPa (Barford & Johnson, 1989), is a global 5° rotation of each subunit about an axis intersecting and approximately orthogonal to the dyad (*p*) axis of the dimer. As a result of this rotation, the catalytic sites of the two subunits move apart and thereby dislodge a reverse-turn segment of polypeptide chain (residues 278–289) that blocks the active site of each subunit. In the T-state, the gate is stabilized by contacts between the tower helix ($\alpha 7$: residues 264–277) and its dyad (*p*-axis)-related counterpart. The subunit rotations that occur on transition to the R-state are accompanied by an 80° change in the packing angle between the tower helices and a concomitant transition of the gate to a disordered state. However, crystal soaking experiments with GCP demonstrated that substrate binding alone could induce partial disorder in the gate in the absence of significant quaternary structural changes (Withers et al., 1982a).

The PLPP-GPb subunit also differs from T-state conformers by a 5° increase in the angular separation between the carboxy (C)- and amino (N)-terminal domains (as defined by their respective β-sheets) (Sprang et al., 1991). A similar, but much smaller structural change was described in crystals of T-state glucose-inhibited phosphorylase a after prolonged exposure to a solution containing phosphate and maltoheptaose (Goldsmith et al., 1989b). The magnitude of the domain rotation with respect to the nucleotide binding motif (residues 560–720) is shown graphically in Figure 3 and schematically in Figure 4 and Kinemage 1. In phosphorylase, unlike many other bilobal enzymes (Bennett & Huber, 1981), the constituent domains rotate apart rather than together when substrates are bound.

Although the four subunits show rms positional differences of ca. 0.6 Å after superposition of all corresponding Cα atoms, the nucleotide binding motifs (Rao & Rossmann, 1973) of the four subunits can be superimposed with an rms deviation of only 0.35 Å, which is within the precision of the structure determination. Superposition of the nucleotide binding motifs of the PLPP-GPb subunits with those of the T-state glucose-inhibited GPa gives rms positional differences of only 0.4 Å, with global displacements of several angstroms in other regions of the struc-

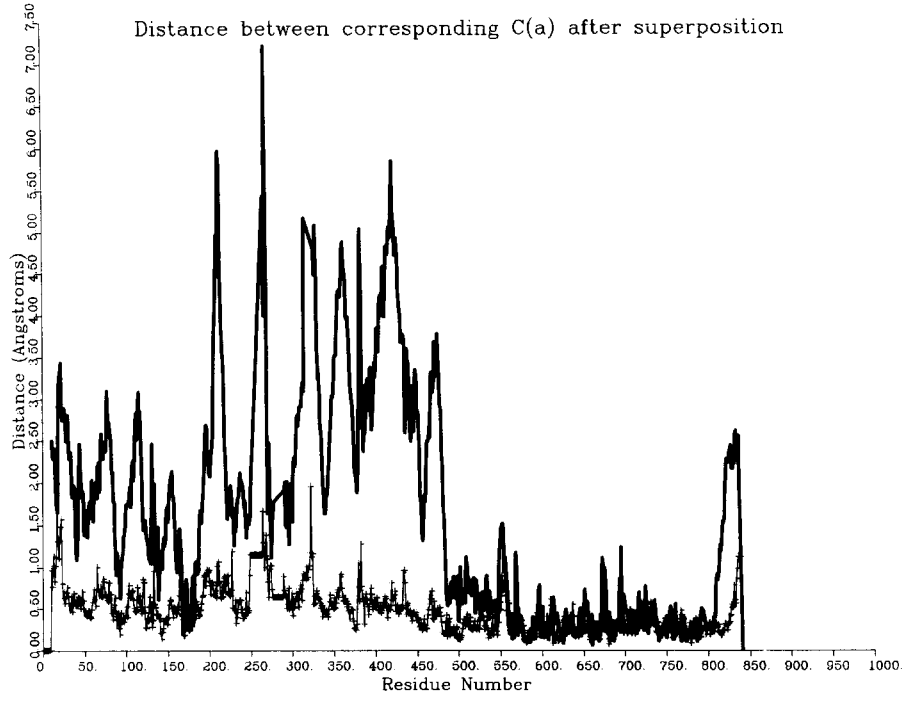

Fig. 3. A plot showing the differences among subunits in comparison to the differences between T and R forms. The solid line shows the displacement (Å) between corresponding Cα atoms after superposition of a subunit of the T-state glucose-GPa complex upon subunit A of PLPP-GPb. The plus signs show the mean displacement of B, C, and D after superposition onto subunit A. The subunits were superimposed using the 160 Cα atoms of residues 560–720, which define the approximate boundary of the nucleotide binding domain in GP.

ture (Fig. 4a). The $(\beta\alpha\beta\alpha\beta)\alpha(\beta\alpha\beta\alpha\beta)$ nucleotide binding domain core of the C-terminal domain behaves as a rigid body in the T → R transition. The superpositions also show that the four PLPP-GPb subunits differ slightly with respect to relative orientation between their amino- and carboxy-terminal domains (Figs. 3, 4b). It is likely that these differences result from nonequivalent environments of the subunits in the crystal lattice. However, it may also be inferred that these variations reflect the dynamic range of conformational states accessible to the phosphorylase subunit and suggest the possibility that breathing motions may play a role in catalysis.

Structural changes within the catalytic site

The deformation of the catalytic site on transition from the glucose-inhibited state of GPa to the pseudo-substrate-bound state of PLPP-GPb is shown in Figure 5 and Kinemage 2. The two structures are shown after superposition of the 160 Cα atoms of the nucleotide binding domains. In the PLPP-GPb crystals, the entire polypeptide chain from residues 277–289 is disordered and is not visible in the electron density maps. In glucose-inhibited GPa and in T-state GPb, these gate residues form a barrier between the catalytic site and the solvent. In the T-state, the gate forms several interactions with residues of the N- and C-terminal domains and thereby serves to stabilize the closed conformation of the subunit. All of these interactions are disrupted in PLPP-GPb, thereby relaxing the structural restraints that keep the domains together in the T-state. A single helical turn (residues 380–384), at the mouth of the catalytic site shifts more than 5 Å away from the C-terminal domain on transition to the R-state. This movement contributes to the opening of the catalytic site and disrupts an ionic link (Glu 382 to Arg 770) between the N- and C-terminal domains.

Model-building experiments were performed to determine whether the interactions observed between glucosyl substrate analogs in the T-state can be maintained in an R-state active site conformation similar to that of the PLPP-GPb. Superpositions of the PLPP-GPb enzyme with glucose, GCP, and G-1-P were constructed to generate rough models of the reactive complex formed by the glucosyl moiety of the oligosaccharide substrate with the phosphate substrate (as represented by the terminal PLPP phosphate) in the R-state enzyme. Crystallographic studies of the complexes formed by GPa with glucose (Sprang et al., 1982) and GCP (Withers et al., 1982b) showed that the glucosyl moiety contacts groups in both the N- and C-terminal domains. These include side chain atoms in Asn 284, His 377, Asn 484, and Glu 672 and the main chain atoms of Ala 673, Ser 674, and Gly 675. The site at which a glycosyl moiety might bind to the R-state enzyme can be modeled by superimposing the coordinates of the GPa complexes onto those of PLPP-GPb. If the nucleotide binding domains of the T and R conformations are superimposed as shown in Figure 5, the glucosyl group is able to maintain contacts with residues 673–675 in the C-terminal domain, but the hydrogen-bond geometry with His 377 and Asn 484 in the N-terminal domain of PLPP-GPb is slightly less favorable than in the GPa complex with glucose. Alternatively,

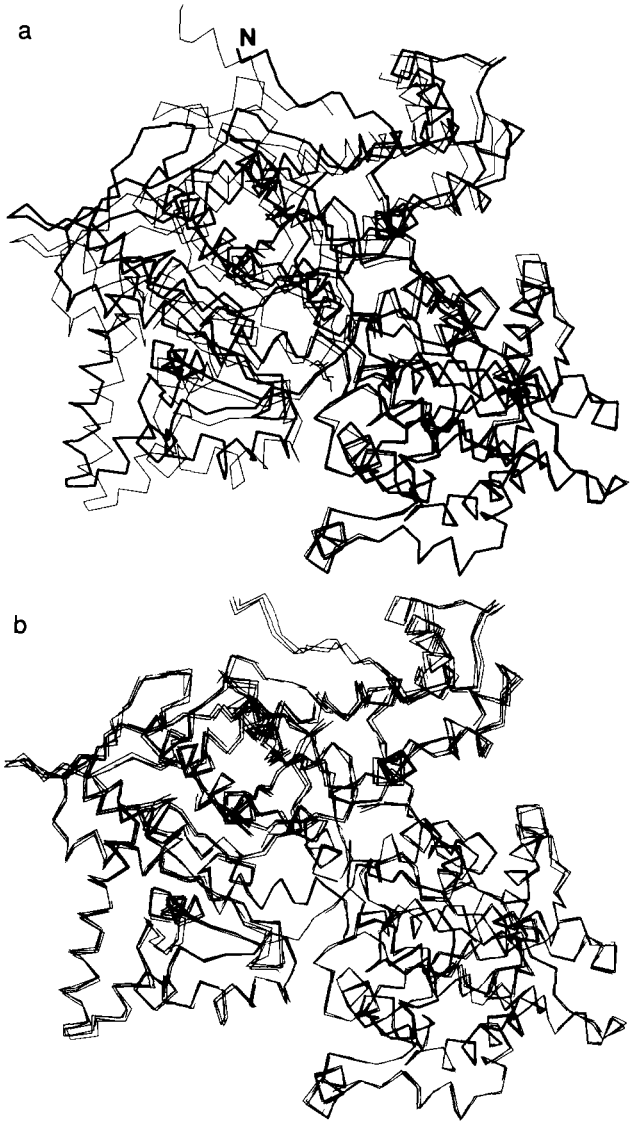

Fig. 4. **a**: A Cα trace of subunit A of PLPP-GPb after superposition of its nucleotide binding motif (residues 560–720) on that of T-state glucose-inhibited GPa as described in the legend to Figure 3; the amino (N)-terminus is labeled. **b**: A Cα trace of subunits A–D of PLPP-GPb after superposition of their nucleotide binding motifs.

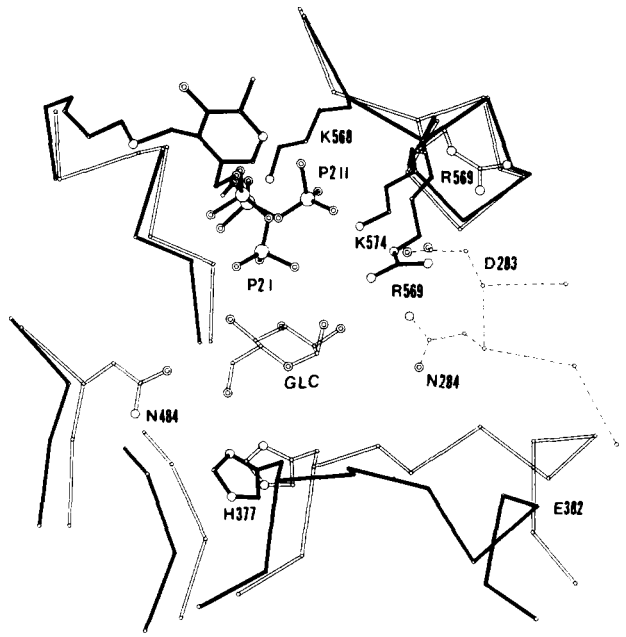

Fig. 5. The active site of PLPP-GPb subunit A (darkened bonds) superimposed upon that of glucose-inhibited GPa (empty bonds). Glucose is shown with open bonds. The dashed lines show the position of residues 282–286 of the gate. These residues are disordered in PLPP-GPb The view is taken approximately perpendicular to the dyad axis of the dimer (*p*), looking down from the subunit interface (along *q*). Both the protein and glucose atoms of GPa have been superimposed onto PLPP-GPb using the Cα atoms of the nucleotide binding motif (residues 560–720).

if the glucosyl position is modeled by a transformation that superimposes residues 360–370 and 460–480, the contacts to 377 and 484 are maintained, whereas those to Ser 674 and Gly 675 are slightly less favorable (Fig. 6a). In the latter model the glucosyl group is slightly closer to the PLP phosphate than in the T-state complex with GPa (compare Figs. 5 and 6a), but both superpositions accommodate the glucosyl-enzyme contacts observed in the T-state. The results of the model-building experiments are consistent with the view that similar contacts are formed between the enzyme and its glucosyl substrate in the R- and T-states.

Superposition of GPa and PLPP-GPb using residues in the nucleotide binding fold (Fig. 5) shows that residues that form direct interactions to the pyridoxal phosphate moiety do not undergo large movements on transition to the R-state. However, the PLP moiety itself rotates away from the glucose binding site, causing the 5′ phosphate to move about 1–1.5 Å away from the C-terminal domain components of the catalytic site (residues 568–573 and 672–677). Consequently, the ion pairs formed by Lys 568 and Lys 574 to the PLP 5′ phosphate in the T-state are not made with the P1 phosphate group in the PLPP-GPb crystals (Table 2). Indeed, it was proposed that such interactions become stronger in the R-state (Withers et al., 1981b, 1985) suggesting that the coenzyme phosphate is present as a constrained dianion. However, it should be noted that the P1 phosphate of PLPP can only be monoanionic and thus will not form the same number of strong interactions as may be present in the native R-state enzyme.

Conformational disorder of the PLPP beta phosphate

The terminal phosphate of the PLPP coenzyme analog adopts two positions in subunits A and C of the PLPP-GPb tetramer (Figs. 1, 5, 6; Kinemage 3). The two conformations differ principally in the torsion angles about

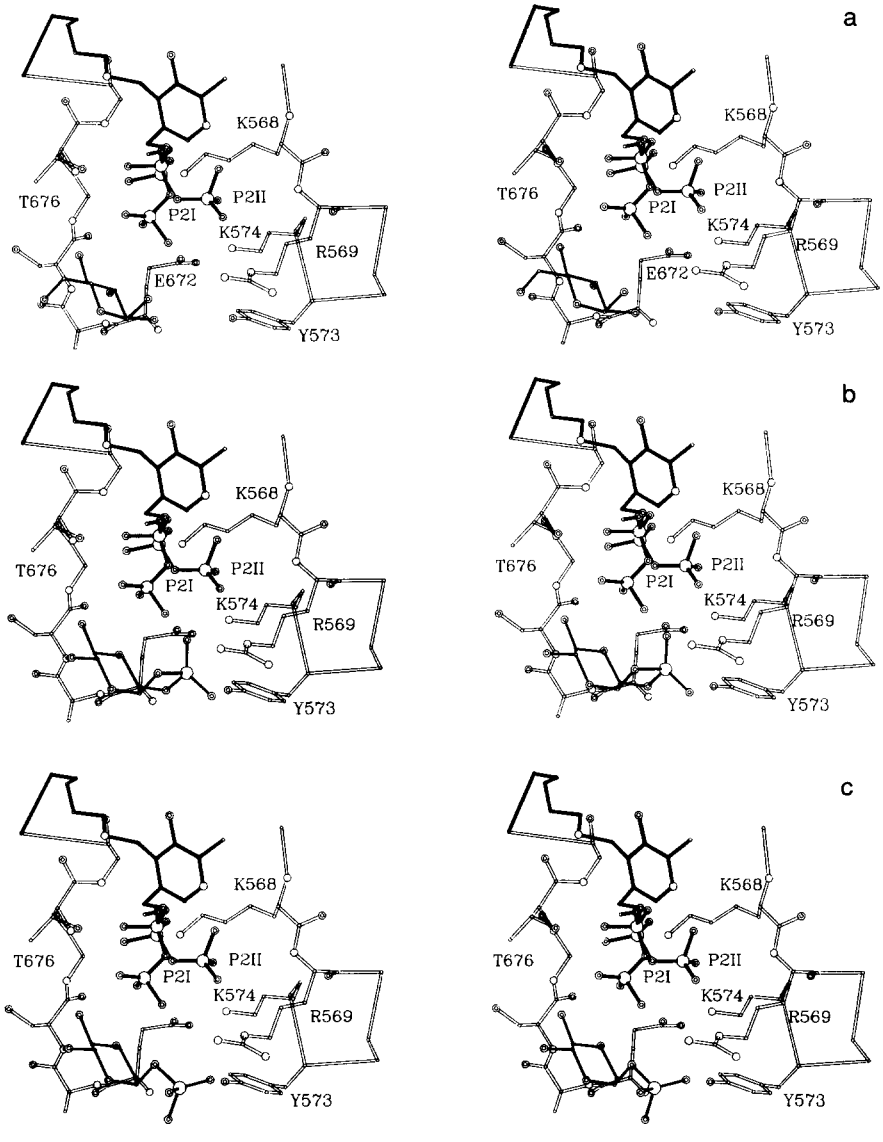

Fig. 6. The environment of the PLPP in subunit A of PLPP-GPb. The darkened bonds depict the two positions (P2I and P2II) of the disordered coenzyme analog. **a**: α-D-glucose, from the glucose-inhibited GPa structure (Sprang et al., 1988) is shown with thin, darkened bonds. Glucose is superimposed onto the PLPP-GPb active site using the transformation that superimposes the Cα atoms of residues 370–380 and 470–485 of GPa onto the corresponding atoms of PLPP-GPb. **b**: GCP substrate analog, determined by difference Fourier analysis of T-state GPa crystals soaked in buffer solution containing the analog (Withers et al., 1982b), is shown in thin black bonds. **c**: A model of G-1-P obtained by rotating the O5-C1-O1-P torsion angle of GCP (above) to 90°.

the two phosphodiester linkages to the P1 phosphate group (Table 3). In conformation I, the P2 phosphate is positioned near the main chain atoms of Gly 675, closest to the glucosyl binding site, whereas in conformation II, it is adjacent to the main chain atoms of Arg 569. The P2I–P2II distance is 2.5–3 Å. The two conformations appear to be equally occupied in subunits A and C, whereas only conformations I and II, respectively, are observed in subunits B and D. The electron density for the P2 phosphate is not well defined in any of the four subunits (Fig. 1), and consequently it is not possible to describe the interactions between that group and the residues in the catalytic site with accuracy. In particular, interactions with the disordered Arg 569 are poorly defined. The P2II position is the closest (ca. 3 Å) to that occupied by the carboxylate of Asp 283 in the T-state (Fig. 5). Repulsive electrostatic interactions between the P2II phosphate and Asp 283 would clearly destabilize the T-state conformation of the gate. The P2II position appears to be similar to the single P2 position observed in PLPP-GPb crystals grown from ammonium sulfate in the presence of IMP (Leonidas et al., 1992).

The positions of both P2I and P2II phosphates are distinct from those occupied by orthophosphate (Goldsmith et al., 1989b) and the 1,2-phosphate of GCP (Withers et al., 1982a) in complexes with T-state GPa. The O1–P phosphodiester bond of GCP adopts the sterically strained (O5-C1-O1-P torsion angle, $\phi = 200°$) conformation imposed by the covalent linkage between P and O2′, in contrast to the more extended conformation favored by G-1-P ($\phi = 90°$). Heptulose 2-phosphate, the product of the phosphorolysis of heptenitol, was found to bind at the active site in the same strained conformation in crystals of GPb (McLaughlin et al., 1984; Johnson et al., 1990). A superposition of GCP onto the structure of the PLPP-GPb complex is shown in Figure 6b and

Table 2. *Hydrogen bonds and polar contacts to phosphate oxygens in PLPP-GPb and in glucose-GPa*[a]

Atom	Subunit A I	Subunit A II	Subunit B I	Subunit C I	Subunit C II	Subunit D II	GPa
OB1	–	–	T676 OG1	–	–	**T676 OG1**	**K574 NZ**
	G677 N	G677 N	G677 N	G677 N	G677 N	**G677 N**	–
O11	V567 O	V567 O	V567 O	–	V567 O	–	–
	K568 NZ	K568 NZ		**K568 NZ**	K568 NZ	**K568 NZ**	–
O12	–	–	**K568 NZ**	–	–		–
	T676 N	**T676 N**	T676 N	**T676 N**	T676 N		**T676N**
	T676 OG	T676 OG		**T676 OG**	T676 OG		
	G677 N	**G677 N**	G677 N	**G677 N**	G677 N		**G677 N**
	–	–	N678 OD1	–	–		–
OB2	–	–	–	–	–	–	**K568 NZ**
O21	–	–	K568 NZ	K568 NZ	**K568 N**	–	
	–	**R569 NE**	–	–	–	**R569 NH1**	
	–	–	–	–	–	**R569 N**	
	T676 OG1	–	–	–	–	–	
O22	–	–	–	–	–		
	–	R569 N	R569 NH2	–	–	**R569 NH1**	
		K574 NZ	–	–	–	–	
O23			–	–	R568 NZ	**R569 NH2**	
	R569 NE	R569 N	–	–	–	–	
	–	–	–	–	**K574 NZ**	**K574 NZ**	
	–	–	G675 N	–	–	–	
	–	–	T676 N	T676 N	–	–	
	–	–	**T676 OG1**	T676 OG1	–	–	

[a] Contacts less than 4.0 Å are tabulated. Contacts less than 3.3 Å are shown in bold. Roman numerals refer to PLPP conformer.

Kinemage 3. The phosphate group of GCP in this model is located about 4.5 Å from P2I, and the anomeric carbon of GCP and its oxygen substituent are 4.0 Å and 3.1 Å, respectively, from the nearest P2I oxygen atom. On this basis, it is reasonable to suppose that the phosphate substrate, poised to donate a proton to the glycosidic oxygen of an oligosaccharide substrate, might bind at a position near that defined by the P2I phosphate in PLPP-GPb.

A model of the PLPP-GPb complex with G-1-P complex is easily obtained by rotating the phosphate group of GCP in the above model to the $\phi = 90°$ conformation (Fig. 6c; Kinemage 3). The glucosyl phosphate in this model is within 1.5 Å of the site at which orthophosphate is bound in the crystals of the partially activated GPa–maltoheptaose–phosphate complex (Goldsmith et al., 1989b).

Table 3. *Conformation about the PLPP phosphodiester atoms*[a]

PLPP group	C4	C5	C5A	OB1	P1	OB2	P2	O21
A I		93	152	−70	113	−60		
A II		74	123	0	108	67		
B I		99	150	−66	161	38		
C I		82	106	52	−123	−43		
C II		93	160	−59	−94	140		
D II		88	127	−43	126	45		

[a] Angles in degrees are shown beneath the bond that defines the torsion angle in the series: C4-C5-C5A-OB1-P1-OB2-P2-O21. See Figure 1B for atom name convention.

Discussion

The AMP complex of PLPP-GPb is a covalently stabilized analog of a reaction intermediate in which the substrate and coenzyme phosphate groups are in close proximity. Both the electrophilic and proton-shuttle mechanism require such an approximation within a ternary complex consisting of the glucosyl ring, the attacking phosphate, and the coenzyme phosphate. The structure described in this report is that of the enzyme in the catalytically active R-state. This is suggested both by the formation of tetramers in solution, which is also manifested in the crystal lattice, and the evidence of conformational differences with respect to T-state crystal forms of GPa and GPb (Sprang et al., 1991). AMP was also shown to lock PLPP-GPb in the R-state conformation by solution studies (Withers et al., 1982b). The quaternary transition from the T-state observed in PLPP-GPb is similar to that described in a different crystal form of GPb in which the R-state is stabilized by sulfate ions at the serine-phosphate and AMP effector sites and at the catalytic site (Barford & Johnson, 1989).

The disposition of the coenzyme analog pyrophosphoryl group within the active site provides no direct evidence to favor one of the two mechanistic models de-

scribed above over the other. By virtue of the covalent attachment of the two phosphates, PLPP-GPb is inherently a better analog of the proposed transition state in the electrophilic mechanism, in which the PLP-phosphate is distorted into a trigonal-bipyramidal configuration to which the substrate phosphate is bound as the apical ligand (Withers et al., 1981b).

PLPP adopts two conformations within the catalytic site. The P2I conformer, which is close to the position occupied by the glucosyl ring in T-state complexes of GPa (Sprang et al., 1982), may mimic the substrate phosphate at or near the transition state of the reaction in either of the proposed mechanisms. The glucosyl phosphate binding site can be modeled by superposition of GCP, a potent competitive inhibitor of G-1-P (Withers et al., 1981a), into the active site of PLPP-GPb. By virtue of its covalent structure, GCP adopts a strained conformation about its O1-P bond, which is similar to that of heptenitol 2-phosphate bound to the catalytic site of GPb (McLaughlin et al., 1984; Johnson et al., 1990). Johnson et al. (1990) suggest that the strained conformation about the O1-P bond would be predicted by stereoelectronic theory to promote cleavage of the α-glycosidic bond; they propose that the natural substrate, G-1-P, adopts a similar conformation as a reactive intermediate in the catalytic mechanism. The P2I phosphate oxygen atom of PLPP lies within 3.5 Å of that modeled for the C1 carbon atom of GCP and is approximately positioned to protonate the glycosidic oxygen of the oligosaccharide substrate and for subsequent nucleophilic attack on the anomeric carbon of the carbonium ion intermediate. The very close approximation of the pyrophosphoryl group of PLPP to the anomeric carbon in this model meets the stereochemical requirements of the electrophilic mechanism. However, the model provides no evidence against a proton shuttle mechanism in which the PLP 5′-phosphate acts as a general acid/base.

It is noteworthy that the P2I phosphate is approximately 4 Å from the carboxylate of Glu 672, suggesting a possible role for that residue in a proton transfer mechanism. However, the Glu 672 carboxylate does not appear to be properly oriented to stabilize the glucosyl carbonium ion intermediate that would follow from either the electrophilic or proton-transfer mechanisms. Indeed, as has been noted earlier (McLaughlin et al., 1984; Johnson et al., 1990), there is no residue in the catalytic site of the PLPP-GPb enzyme positioned to stabilize a putative carbonium ion intermediate, suggesting, as proposed by Klein et al. (1986) and Palm et al. (1990), that the substrate phosphate itself performs that function as a mobile anion. However, it should be noted that no oligosaccharide is present in this structure, and it is well known (Cohn & Cori, 1948) that no half reactions with the natural substrate occur in the absence of oligosaccharide. Binding of the oligosaccharide may well be accompanied by conformational changes that result in relocalization of catalytic groups that are not properly positioned in the unliganded or partially ligated states of the enzyme. Mutagenesis experiments with the *Escherichia coli* enzyme (Schinzel & Palm, 1990) indicate that Glu 672 is involved in substrate binding in the transition state rather than in the ground state complex.

The II conformation of the pyrophosphoryl moiety places the P2 phosphate next to the main chain atoms of Arg 569. The P2 phosphate in this conformation is not well disposed for an attack upon the glucosyl ring. It is possible that the substrate phosphate binds to a site near this position to form a prereaction ternary complex (in the direction of glycogen phosphorolysis). A reaction mechanism can be envisioned in which the substrate phosphate is in transit from the prereaction (E·S) site II to the reactive I site at which nucleophilic attack occurs. Such a scheme is consistent with a rapid equilibrium random-bimolecular kinetic mechanism of glycogen phosphorylase in which a prereaction tertiary complex is formed (Engers et al., 1969, 1970; Gold et al., 1970).

Lastly, the orthophosphate bound to GPa (Goldsmith et al., 1989b) defines a third distinct substrate phosphate site. The phosphate bound at this position is close to the entrance to the catalytic site and is located 7 Å away from the 5′-phosphate of the PLP. The phosphate of GCP, as modeled in the active site of PLPP-GPb can be nearly superimposed onto the orthophosphate position by rotation to the $\phi = 90°$ conformation favored by G-1-P, the product (or the substrate in the direction of glycogen synthesis) of the reaction catalyzed by GP. The three phosphate positions observed in the crystal structures of PLPP-GPb and of the complex of orthophosphate with GPa may conform roughly to distinct phosphate subsites occupied at successive stages in the catalytic mechanism (Fig. 7). In such a mechanism, Arg 569 could act as a mobile cationic ligand, tracking the phosphate as it transits between sites. Indeed, Arg 569 is disordered in PLPP-GPb. Substitution of the residue corresponding to Arg 569 nearly abolishes the catalytic activity of the *E. coli* maltodextrin phosphorylase (Schinzel & Drueckes, 1991). The mobility of the substrate phosphate may be facilitated by the flexibility of the hinge region connecting the C-terminal domain of the enzyme (to which the PLP is bound) to the N-terminal domain (which contains binding residues for the glycosyl moiety and the substrate phosphate). The distribution of hinge conformers observed among the four PLPP-GPb subunits in the tetramer may be representative of the dynamic range of the breathing motions accessible to the R-state enzyme, and it is possible that such flexibility is a necessary and intrinsic property of the R-state of phosphorylase. Indeed the active R-state must accommodate various conformational changes occurring during each catalytic cycle, and these nonallosteric changes may be quite large, as demonstrated by the hexokinase monomer (Anderson et al., 1979).

The relevance of the PLPP-GPb structure to that of the E·S complex or the transition state is subject to at least two caveats. First, the P2 phosphate is covalently

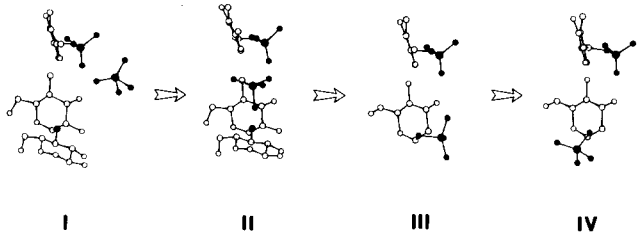

Fig. 7. A schematic diagram showing hypothetical binding sites for the substrate phosphate group at different points along the reaction coordinate for the glycogen phosphorylase-catalyzed phosphorolysis of α-D-(1-4)-linked oligoglucoside substrates. The subsites correspond approximately to phosphate binding sites observed in PLPP-GPb and in the complexes of orthophosphate (Goldsmith et al., 1989b) and GCP (Withers et al., 1982b) with GPa. The stereochemical mechanism is assumed only to require close approximation between the substrate and PLP 5′-phosphate group, but implies no particular chemical mechanism, nor is any particular orientation of the substrate phosphate intended. The view is shown along the plane of the pyridoxal ring of the PLP coenzyme at the top of each panel. The phosphate groups of the PLP and substrate phosphate are darkened, as is the glycosyl oxygen of the disaccharide substrate. In panel I, the ternary complex of the enzyme with the orthophosphate and oligosaccharide is shown. The phosphate is bound at a site corresponding to P2II of PLPP-GPb (see text). Panel II shows the orthophosphate translated to a site near P2I in a hypothetical activated complex. Panel III shows the G-1-P product in the strained conformation observed for GCP in GPa (858) and heptulose-2-phosphate in GPb (Johnson et al., 1990). In panel IV, the phosphate group of G-1-P is rotated to the unstrained, extended conformation where it is positioned close to the site occupied by orthophosphate in GPa (Withers et al., 1982b).

constrained, thus the position(s) it occupies in the catalytic site may be a fortuitous consequence of the covalent linkage. Second, the structure of the ternary complex of the enzyme with its natural substrates (G-1-P or phosphate with oligosaccharide) has not yet been determined. A realistic picture of the stereochemical events that occur on the reaction pathway catalyzed by glycogen phosphorylase must await the structural analysis of true analogs of the ternary complex.

Materials and methods

The preparation of PLPP-GPb (Withers et al., 1981a) has been described. Crystals of PLPP-GPb were obtained using polyethylene glycol 8000 as a precipitant in the presence of 0.5 mM AMP and 12.5 mM maltoheptaose (Sprang et al., 1991). X-ray data measurement and determination of the structure of PLPP-GPb have been reported (Sprang et al., 1991). In this study the crystallographic refinement has been extended to include all of the measured data to a resolution of 2.87 Å. It was evident upon examination of the electron density maps computed with data to 3.0 Å that the terminal phosphate of the PLPP residue exhibited two conformations in at least two of the four subunits. Positions for the PLPP conformers were defined by fitting the PLPP model, with appropriate adjustment of phosphodiester bonds, into a simulated annealing omit map calculated with the program X-PLOR (Brünger, 1990). In this procedure, all atoms within a 6-Å radius of any atom within (and including) the PLPP are excluded from the phasing during a run of molecular dynamics in which a 3.0-Å shell of atoms around the excluded region is fixed by harmonic restraints. This procedure minimizes the phase bias introduced by the position of the PLPP in previous models. Even though the alternative PLPP conformations appeared to differ mainly in the values of two torsion angles about the P1 phosphate (see Fig. 1 for numbering convention), the entire PLPP group was chosen to comprise the statistically disordered unit. Both PLPP conformers were included in the structure factor calculation even though, within a single refinement run, the coordinates of only one of the PLPP positions were subject to refinement. Nonbonded interaction terms between the two PLPP positions were omitted from the set of stereochemical constraints, so that each of the two PLPP positions were, in effect, refined independently. Two rounds of positional refinement of all nonhydrogen atoms in the atomic model were conducted, each round incorporating one of the two disordered PLPP positions (memory allocation constraints prevented the refinement of both disordered PLPP positions in a single round of refinement). These were followed by a single cycle of constrained temperature factor refinement of all atoms. No noncrystallographic symmetry constraints were imposed on the four subunits in the asymmetric unit. No water molecules were included in the refinement. Atomic coordinates for PLPP-GPb have been deposited as entry 1PYG in the Protein Data Bank (Chemistry Department, Brookhaven National Laboratory, Upton, New York 11973).

Acknowledgments

We thank S. Shechosky for technical assistance and E. Goldsmith for a critical reading of the manuscript. This research was supported in part by NIH research grant R01 DK31507 (S.R.S.), grant I1229 from the Welch Foundation, the Natural Sciences and Engineering Research Council of Canada (S.G.W.), and the Medical Research Council of Canada (N.B.M.)

References

Acharya, K.R., Stuart, D.I., Varvill, K.M., & Johnson, L.N. (1991). *Glycogen Phosphorylase b: Description of the Protein Structure*, pp. 1-123. World Scientific Publishing Co. Pte. Ltd., Singapore.

Anderson, C.M., Zucker, F.H., & Steitz, T.A. (1979). Space-filling models of kinase clefts and conformational changes. *Science 204*, 375-380.

Barford, D., Hu, S.-H., & Johnson, L.N. (1991). Structural mechanism for glycogen phosphorylase control by phosphorylation and AMP. *J. Mol. Biol. 218*, 233-260.

Barford, D. & Johnson, L.N. (1989). The allosteric transition of glycogen phosphorylase. *Nature 340*, 609-616.

Barford, D. & Johnson, L.N. (1992). The molecular mechanism for the tetrameric association of glycogen phosphorylase promoted by protein phosphorylation. *Protein Sci. 1*, 472-493.

Bennett, W.S. & Huber, R. (1981). Structural and functional aspects of domain motions in proteins. *CRC Crit. Rev. Biochem. 15*, 291-384.

Brünger, A.T. (1990). *X-PLOR (Version 2.1) Manual*. Yale University, New Haven.

Buc, H. (1967). On the allosteric interaction between 5'AMP and orthophosphate on phosphorylase b. Quantitative kinetic predictions. *Biochem. Biophys. Res. Commun. 28*, 59–64.

Cohn, M. & Cori, G.T. (1948). On the mechanism of action of muscle and potato phosphorylase. *J. Biol. Chem. 175*, 89–93.

Engers, H.D., Bridger, W.A., & Madsen, N.B. (1969). Kinetic mechanism of phosphorylase *b*. *J. Biol. Chem. 244*, 5936–5942.

Engers, H.D., Shechosky, S., & Madsen, N.B. (1970). Kinetic mechanism of phosphorylase *a*. I. Initial velocity studies. *Can. J. Biochem. 48*, 746–754.

Fischer, E.H., Kent, A.B., Snyder, E.R., & Krebs, E.G. (1958). The reaction of sodium borohydride with muscle phosphorylase. *J. Am. Chem. Soc. 80*, 2906–2907.

Fletterick, R.J. & Madsen, N.B. (1980). The structures and related functions of phosphorylase *a*. *Annu. Rev. Biochem. 49*, 31–61.

Gold, A.M., Johnson, R.M., & Tseng, J.K. (1970). Kinetic mechanism of rabbit muscle glycogen phosphorylase *a*. *J. Biol. Chem. 245*, 2564–2572.

Goldsmith, E.J. & Fletterick, R.J. (1983). Oligosaccharide conformation and protein saccharide interactions in solution. *Pure Appl. Chem. 55*, 577–588.

Goldsmith, E., Sprang, S., & Fletterick, R. (1982). Structure of maltoheptaose by difference Fourier methods and a model for glycogen. *J. Mol. Biol. 156*, 411–427.

Goldsmith, E.J., Sprang, S.R., & Fletterick, R.J. (1989a). Alternative binding modes for maltopentaose in the activation site of glycogen phosphorylase a. *Trans. Am. Crystallogr. Soc. 25*, 87–104.

Goldsmith, E.J., Sprang, S.R., Hamlin, R., Xuong, N.-H., & Fletterick, R.J. (1989b). Domain separation in the activation of glycogen phosphorylase a. *Science 245*, 528–532.

Graves, D.J. & Wang, J.H. (1972). α-Glucan phosphorylases—Chemical and physical basis of catalysis and regulation. In *The Enzymes* (Boyer, P.D., Ed.), pp. 435–482. Academic Press, New York.

Helmreich, E.J.M. & Klein, H.W. (1980). The role of pyridoxal phosphate in the catalysis of glycogen phosphorylases. *Angew. Chem. Int. Ed. Engl. 19*, 441–445.

Johnson, L.N., Acharya, K.R., Jordan, M.D., & McLaughlin, P.J. (1990). Refined crystal structure of the phosphorylase-heptulose 2-phosphate-oligosaccharide-AMP complex. *J. Mol. Biol. 211*, 645–661.

Johnson, L.N., Cheetham, J., McLaughlin, P.J., Acharya, K.R., & Phillips, D.C. (1988). Protein-oligosaccharide interactions: Lysozyme, phosphorylase, amylases. *Curr. Top. Microbiol. Immunol. 139*, 81–134.

Kasvinsky, P.J., Madsen, N.B., Fletterick, R.J., & Sygusch, J. (1978a). X-ray crystallographic and kinetic studies of oligosaccharide binding to phosphorylase. *J. Biol. Chem. 253*, 1290–1296.

Kasvinsky, P.J., Madsen, N.B., Sygusch, J., & Fletterick, R.J. (1978b). The regulation of glycogen phosphorylase a by nucleotide derivatives. *J. Biol. Chem. 245*, 3343–3351.

Klein, H.W., Im, M.J., & Palm, D. (1986). Mechanism of the phosphorylase reaction. *Eur. J. Biochem. 157*, 107–144.

Klein, H.W., Palm, D., & Helmreich, J.M. (1982). General acid-base catalysis of α-glucan phosphorylases: Stereospecific glucosyl transfer from D-glucal is a pyridoxal 5'phosphate and orthophosphate (arsenate) dependent reaction. *Biochemistry 21*, 6675–6684.

Leonidas, D.D., Oikonomakos, N.G., Papageorgiou, A.C., Acharya, K.R., Barford, D., & Johnson, L.N. (1992). Control of phosphorylase *b* by a modified cofactor: Crystallographic studies on R-state glycogen phosphorylase reconstituted with pyridoxal 5'-diphosphate. *Protein Sci. 1*, 1112–1122.

Lorek, A., Wilson, K.S., Sansom, M.S.P., Stuart, D.I., Stura, E.A., Jenkins, J.A., Zanotti, G., Hajdu, J., & Johnson, L.N. (1984). Allosteric interactions of glycogen phosphorylase *b*. *Biochem. J. 218*, 45–60.

Luzzati, P.V. (1952). Traitement statistique de erreurs dans la determination des structures cristallines. *Acta Crystallogr. 5*, 802–810.

McLaughlin, P.J., Stuart, D.I., Klein, H.W., Oikonomakos, N.G., & Johnson, L.N. (1984). Substrate-cofactor interactions for glycogen phosphorylase *b*: A binding study in the crystal with heptenitol and heptulose 2-phosphate. *Biochemistry 23*, 5862–5873.

Metzger, B., Helmreich, E., & Glaser, L. (1967). The mechanisms of activation of skeletal muscle phosphorylase A by glycogen. *Proc. Natl. Acad. Sci. USA 57*, 994–1001.

Monod, J., Wyman, J., & Changeux, J.-P. (1965). On the nature of allosteric transitions: A plausible model. *J. Mol. Biol. 12*, 88–118.

Newgard, C.B., Hwang, P.K., & Fletterick, R.J. (1989). The family of glycogen phosphorylases: Structure and function. *CRC Crit. Rev. Biochem. 24*, 69–99.

Palm, D., Klein, H.W., Schinzel, R., Buehner, M., & Helmreich, E.J.M. (1990). The role of pyridoxal 5'-phosphate in glycogen phosphorylase catalysis. *Biochemistry 29*, 1099–1106.

Parrish, R.F., Uhing, R.J., & Graves, D.J. (1977). Effect of phosphate analogues on the activity of pyridoxal reconstituted glycogen phosphorylase. *Biochemistry 16*, 4824–4831.

Pfeuffer, T., Ehrlich, J., & Helmreich, E. (1972). Role of pyridoxal 5'-phosphate in glycogen phosphorylase. II. Mode of binding of pyridoxal 5'-phosphate and analogs of pyridoxal 5'-phosphate to apophosphorylase *b* and the aggregation state of the reconstituted phosphorylase proteins. *Biochemistry 11*, 2135–2145.

Rao, S. & Rossmann, M.G. (1973). Comparison of supersecondary structure in proteins. *J. Mol. Biol. 76*, 241–256.

Schinzel, R. & Drueckes, P. (1991). The phosphate recognition site of *Escherichia coli* maltodextrin phosphorylase. *FEBS Lett. 286*, 125–128.

Schinzel, R. & Palm, D. (1990). *Escherichia coli* maltodextrin phosphorylase: Contribution of active site residues glutimate-637 and tyrosine-538 to the phosphorylytic cleavage of α-glucans. *Biochemistry 29*, 9956–9962.

Shaltiel, S., Hedrick, J.L., Pocker, A., & Fischer, E.H. (1969). Reconstitution of apophosphorylase with pyridoxal 5'-phosphate analogs. *Biochemistry 8*, 5189–5196.

Sprang, S. & Fletterick, R.J. (1979). The structure of glycogen phosphorylase *a* at 2.5 Å resolution. *J. Mol. Biol. 131*, 523–551.

Sprang, S.R., Acharya, K.R., Goldsmith, E.J., Stuart, D.I., Varvill, K., Fletterick, R.J., Madsen, N.B., & Johnson, L.N. (1988). Structural changes in glycogen phosphorylase induced by phosphorylation. *Nature 336*, 215–221.

Sprang, S.R., Goldsmith, E.J., & Fletterick, R.J. (1987). Structure of the nucleotide activation switch in glycogen phosphorylase a. *Science 237*, 1012–1019.

Sprang, S.R., Goldsmith, E.J., Fletterick, R.J., Withers, S.G., & Madsen, N.B. (1982). Catalytic site of glycogen phosphorylase: Structure of the T state and specificity for α-D-glucose. *Biochemistry 21*, 5364–5371.

Sprang, S.R., Withers, S.G., Goldsmith, E.J., Fletterick, R.J., & Madsen, N.B. (1991). Structural basis for the activation of glycogen phosphorylase b by adenosine monophosphate. *Science 254*, 1367–1371.

Takagi, M., Fukui, T., & Shimomura, S. (1982). Catalytic mechanism of glycogen phosphorylase: Pyridoxal(5)diphospho(1)-α-D-glucose as a transition-state analogue. *Proc. Natl. Acad. Sci. USA 79*, 3716–3719.

Wang, J.H., Shonka, M.L., & Graves, D.J. (1965). Influence of carbohydrates on phosphorylase structure and activity I. Activation by preincubation with glycogen. *Biochemistry 4*, 2296–2301.

Withers, S.G., Madsen, N.B., Sprang, S.R., & Fletterick, R.J. (1982a). Catalytic site of glycogen phosphorylase: Structural changes during activation and mechanistic implications. *Biochemistry 21*, 5372–5382.

Withers, S.G., Madsen, N.B., & Sykes, B.D. (1981a). Active form of pyridoxal phosphate in glycogen phosphorylase. Phosphorus-31 nuclear magnetic resonance investigation. *Biochemistry 20*, 1748.

Withers, S.G., Madsen, N.B., & Sykes, B.D. (1982b). Covalently activated glycogen phosphorylase a phosphorus-31 nuclear magnetic resonance and ultracentrifugation analysis. *Biochemistry 21*, 6716–6722.

Withers, S.G., Madsen, N.B., & Sykes, B.D. (1985). ^{31}P NMR relaxation studies of the activation of the coenzyme phosphate of glycogen phosphorylase. *Biophys. J. 48*, 1019–1026.

Withers, S.G., Madsen, N.B., Sykes, B.D., Takagi, M., Shimomura, S., & Fukui, T. (1981b). Evidence for direct phosphate-phosphate interaction between pyridoxal phosphate and substrate in the glycogen phosphorylase catalytic mechanism. *J. Biol. Chem. 256*, 10759–10762.